

Document downloaded from:

<http://hdl.handle.net/10251/202401>

This paper must be cited as:

Torres-Giner, S.; Wilkanowicz, S.; Meléndez-Rodríguez, B.; Lagaron, JM. (2017). Nanoencapsulation of Aloe vera in Synthetic and Naturally Occurring Polymers by Electrohydrodynamic Processing of Interest in Food Technology and Bioactive Packaging. *Journal of Agricultural and Food Chemistry*. 65(22):4439-4448. <https://doi.org/10.1021/acs.jafc.7b01393>



The final publication is available at

<https://doi.org/10.1021/acs.jafc.7b01393>

Copyright American Chemical Society

Additional Information

Nanoencapsulation of Aloe vera in Synthetic and Naturally Occurring Polymers by Electrohydrodynamic Processing of Interest in Food Technology and Bioactive Packaging

Sergio Torres-Giner,[†]Sabina Wilkanowicz,[‡] Beatriz Melendez-Rodriguez,[†] and Jose M. Lagaron^{*,†}

[†] Novel Materials and Nanotechnology Group, Institute of Agrochemistry and Food Technology (IATA), Spanish Council for Scientific Research (CSIC), Calle Catedrático Agustín Escardino Benlloch 7, 46980 Paterna, Spain

[‡]Bioinicia R&D, Calle Algepser 65–Nave 3, Polígono Industrial Tactica, 46988 Paterna, Spain

ABSTRACT: This work originally reports on the use of electrohydrodynamic processing (EHDP) to encapsulate Aloe vera (AV, *Aloe barbadensis* Miller) using both synthetic polymers, i.e., polyvinylpyrrolidone (PVP) and poly(vinyl alcohol) (PVOH), and naturally occurring polymers, i.e., barley starch (BS), whey protein concentrate (WPC), and maltodextrin. The AV leaf juice was used as the water-based solvent for EHDP, and the resultant biopolymer solution properties were evaluated to determine their effect on the process. Morphological analysis revealed that, at the optimal processing conditions, synthetic polymers mainly produced fiber-like structures, while naturally occurring polymers generated capsules. Average sizes ranged from 100 nm to above 3 μ m. As a result of their different and optimal morphology and, hence, higher AV content, PVP, in the form of nanofibers, and WPC, of nanocapsules, were further selected to study the AV stability against ultraviolet (UV) light exposure. Fourier transform infrared (FTIR) spectroscopy confirmed the successful encapsulation of AV in the biopolymer matrices, presenting both encapsulants a high chemical interaction with the bioactive components. Ultraviolet–visible (UV–vis) spectroscopy showed that, while PVP nanofibers offered a poor effect on the AV degradation during UV light exposure (~10% of stability after 5 h), WPC nanobeads delivered excellent protection (stability of >95% after 6 h). This was ascribed to positive interactions between WPC and the hydrophilic components of AV and the inherent UV-blocking and oxygen barrier properties provided by the protein. Therefore, electrospraying of food hydrocolloids interestingly appears as a novel potential nanotechnology tool toward the formulation of more stable functional foods and nutraceuticals.

Keywords: electrospinning, electrospraying, biopolymers, Aloe vera leaf juice, encapsulation, food technology, bioactive packaging

INTRODUCTION

Aloe barbadensis Miller is one of the main species of Aloe vera (AV), which belongs to the family Liliaceae, and its history dates back to the 4th century B.C.¹ The term “aloe” derives from “alloe” in Arabic and “halal” in Hebrew, which means bitter shiny substance, while the epithet “vera” means true or genuine.² The plant of AV is endemic to hot and dry world areas, such as the Arabian Peninsula or Africa, and it is welladapted to grow in desert or arid climates. Therefore, its tissues have highly evolved for the retention and storage of water by the formation of a dense gel, the so-called leaf juice, which contains approximately 0.985 g of water/g wet basis.³

Some of the functional properties of AV are related to its antioxidant activity, wound and burn healing, pain and edema reduction, digestion, and immune response.⁴ There are also some technical reports about its antibacterial and antifungal activity, especially in the form of fresh juice, and anticancer properties.⁵ In addition, the extract of AV leaf juice has been reported to lower blood glucose levels in normal and alloxan-induced diabetic mice.⁶ A wide range of bioactive compounds are found in the AV leaves, such as anthraquinones (e.g., aloins A and B), carbohydrates (e.g., pectin, cellulose, glucomannan, and others), enzymes (e.g.,

amylase, lipase, and oxidase), inorganic compounds (e.g., calcium, magnesium, iron, and zinc salts), non-essential and essential amino acids, and vitamins (e.g., vitamins B1, B2, B6, and C, β -carotene, choline, folic acid, and α -tocopherol).^{7,8} In addition, AV contains salicylic acid that, in combination with magnesium, is considered to work together to provide a natural analgesic effect on burns.^{9,10}

Because the degradation of AV bioactive ingredients starts right after harvesting of the plant, both the whole leaf and inner gel fillet need to be rapidly processed into more stable products. Therefore, protection from chemical degradation of AV compounds is of high importance, and the use of encapsulation technologies represent a suitable solution. Various encapsulation technologies have been previously used to protect AV compounds from degradation, such as freeze drying, spray drying, hot-air drying, and coacervation. For instance, AV has been recently encapsulated in polyamide nanoparticles by the emulsion–diffusion technique, followed by freeze drying.¹¹ In another study, similar AV nanocapsules of a triblock copolymer made of poly(ethylene glycol) (PEG) and poly(butylene adipate) (PBA) were also prepared.¹² However, spray drying, freeze drying, and other more conventional or advanced processing technologies often require the use of extremely low or high temperatures, vacuum, or harsh solvents, which may add complexity or may not be scalable.

Electrohydrodynamic processing (EHDP) can result in the potential interest for the AV encapsulation. This novel process, comprising both electrospinning, when producing fibers, and electrospraying, capsules, is a one-step nanotechnological tool of potential application interest in food technology and related areas.¹³ Because of their extremely high trapping efficiency, electrospun and electrosprayed ultrathin structures have been recently proposed for a huge range of bioactive applications,¹⁴ including the stabilization of antioxidants.^{15,16} The main advantage of EHDP over other encapsulation technologies in the field of food-based applications¹⁷ and drug-delivery systems¹⁸ is related to its high efficiency, sustained release capacity, greater thermal, light, and storage stability, and enhanced protection of loaded ingredients from chemical degradation. As a result of the ultrathin size of the electrospun and electrosprayed structures, resultant materials become much easier to handle and can mask unwanted organoleptic characteristics, such as odor and taste (e.g., fish-related ingredients).^{19–21} Another advantage is the use of solvents at “natural atmospheric conditions”, which efficiently preserves the functional condition of the bioactives.¹⁵

In the EHDP technology, a wide range of polymer materials can be potentially used as the protecting encapsulants. These include both natural and synthetic polymers, which can easily produce ultrathin fibers or capsules. EHDP has particularly expanded the use of polysaccharides as encapsulating materials, such as chitosan, alginates, celluloses, starches, or malto- and cyclodextrins,²² as well as proteins, such as whey protein isolate (WPI), whey protein concentrate (WPC), soy protein isolate (SPI), egg albumen, collagen, gelatin, zein, or casein.²³ In relation to food hydrocolloids, WPC deserves particular attention as a result of its valuable dietary supplement and functional food enhancement properties. This protein complex is made from α -lactalbumin (ALA) and β -lactoglobulin (BLG), with isoelectric points of approximately 4.3 and 5.2, respectively.²⁴ Particularly, ALA has 123 amino acid residues, mostly forming α -helices. Alternatively, BLG is composed of 162 amino acid residues, forming eight antiparallel β -sheets and one α -helix chain.^{25,26} This secondary structure particularly leads to the formation of a globular quaternary structure, which can create closed capsules with impenetrable walls. In addition, similar to other food-grade polymers, WPC is water-soluble and creates hydrocolloids that makes it perfect as a nontoxic encapsulant for the encapsulation of functional ingredients of interest in the food industry. Although the high surface tension of water in an air environment, together with the ionization of water molecules at high voltages, typically complicates EHDP, this can be effectively reduced by the addition of surfactants (e.g., sorbitan monolaurate) at a low weight concentration, i.e., 1–2 wt %.²⁷

Previous research works on the use of EHDP to encapsulate AV are mainly based on poly(vinyl alcohol) (PVOH) and limited to the preparation of wound dressings.^{9,10,28,29} For instance, in a recent work, Serincay et

al.²⁹ produced antimicrobial dressings with the capacity to release AV using electrospun PVOH/poly(acrylic acid) (PAA) nanofibers. Similarly, Uslu and Aytimur⁹ prepared biocompatible dressings containing AV in PVOH/polyvinylpyrrolidone iodine (PVP-I)/ PEG nanofibers. These studies have reported the potential use of the AV-loaded electrospun matrices as wound dressings; however, none of these have evaluated the stability of the bioactive or their potential use as functional ingredients when encapsulated in food-grade polymers. The present study describes the encapsulation of AV leaf juice using EHDP with the objective to protect its bioactive compounds and to provide them in a solid form of more added value for the food, pharmaceutical, and cosmetic industries. For this, edible polymers such as barley starch (BS), WPC, and maltodextrin, were used. These food-grade polymers were compared to polyvinylpyrrolidone (PVP) and PVOH, which are synthetic polymers widely employed in the cosmetic and pharmaceutical industry. The EHDP conditions were first optimized, and the morphology of the resultant biopolymer encapsulating systems was examined. Finally, in the selected biopolymer matrices, the encapsulation stability of AV was analyzed.

MATERIALS AND METHODS

Materials. Leaf juice of AV (*A. barbadensis* Miller) was purchased from Laboratorios Farmaceuticos Pejoseca S.L. (Agüimes, Spain) in gel form under the trade name of aloVeria. This was extracted from AV plants in the Canary Islands and presents a purity of 99.6%. PVP, 437190 grade, with an average molecular weight (M_w) of $\sim 1\,300\,000$ g/mol was received as free-flowing fine powder from Sigma-Aldrich S.A. (Madrid, Spain). Modified PVOH with commercial reference B49v7 was purchased from Plasticos Hidrosolubles (Valencia, Spain) in film form. This biopolymer readily fully dissolves in cold water. Pregelatinized BS sodium octenylsuccinate was Lyckeby Keep 92032 obtained from Lyckeby Culinar AB (Fjalkinge, Sweden) and supplied by Trades S.A. (Barcelona, Spain). Heat-stabilized WPC, with ~ 80 wt % protein content, was kindly donated from ARLA Food Ingredients (Viby, Denmark) under the commercial name of Lacprodan DI-8090. Commercial-resistant maltodextrin, namely, Fibersol-2, was supplied by ADM/Matsutani LLC (Clinton, IA, U.S.A.) and distributed by Alifarma (Reus, Spain). All food hydrocolloids were received in the form of white to off-white coarse ground powder. The surfactant, a sorbitan fatty acid ester, was TEGO SML, purchased from Evonik Industries (Wesseling, Germany) in liquid form.

Preparation of Biopolymer Solutions. The AV leaf juice was used as received without further purification. The leaf juice was found to contain, after drying, a total solids content of AV of 2 wt %. As a result of its original high water content and to simplify any potential industrial process (e.g.,

extraction), the leaf juice was used as the base solvent to solubilize the biopolymers. Because different weight contents of each biopolymer were required to achieve the optimal EHDP conditions, the final dry materials ended up having different contents of AV in the encapsulates. A control solution of each biopolymer was also prepared in identical conditions, substituting the AV leaf juice with deionized water. Table 1 summarizes the biopolymer solutions prepared for EHDP, indicating the resultant

Table 1. Weight Content (wt %) of PVP, PVOH, BS, WPC, Maltodextrin, AV Leaf Juice, and Water in the Prepared Solutions for EHDP and Resultant Content of Encapsulated AV in the Biopolymers

encapsulation system	solution content (wt %)			encapsulated AV content (wt %)
	biopolymer	AV leaf juice	water	
PVP	10	0	90	0
PVP + AV	10	90	0	18
PVOH	10	0	90	0
PVOH + AV	10	90	0	18
BS	20	0	80	0
BS + AV	20	80	0	8
WPC	20	0	80	0
WPC + AV	20	80	0	8
maltodextrin	50	0	50	0
maltodextrin + AV	50	50	0	2

content of AV encapsulated. All solutions were prepared at room temperature, i.e., 25 °C, under high stirring conditions, and 1 wt % surfactant was added.

Characterization of Biopolymer Solutions. Prior to EHDP, all biopolymer solutions were characterized in terms of viscosity, surface tension, and conductivity. The apparent viscosity (η_a) was determined at 100 s⁻¹ using a rotational viscosity meter Visco BasicPlus L from Fungilab S.A. (San Feliu de Llobregat, Spain) equipped with a lowviscosity adapter (LCP). The surface tension was measured following the Wilhemy plate method using an EasyDyne K20 tensiometer from Krüss GmbH (Hamburg, Germany). The conductivity was evaluated using a conductivity meter XS Con6 from Lab-box (Barcelona, Spain). All measurements were carried out at room temperature in triplicate.

EHDP. EHDP was conducted using a high-throughput Fluidnatek LE500 pilot line from Bioinicia S.L. (Valencia, Spain). The basic EHDP equipment has a 24 emitter multinozzle injector, a variable high-voltage 0–60 kV power supply, and two pumping systems to potentially carry out coaxial electrospinning or electrospraying. A 5 mL plastic syringe containing the biopolymer solution was placed on one pump and was vertically directed to the collector. A negatively polarized collector was used to drive the solids from the injector to the collector. The different biopolymer solutions containing AV leaf juice and water as solvents were

initially optimized in terms of the flow rate, tip-collector distance, and voltage. Table 2 summarizes the selected

Table 2. Optimal Conditions during EHDP of PVP, PVOH, BS, WPC, and Maltodextrin with and without AV

encapsulation system	flow rate (mL/h)	needle-collector distance (cm)	voltage (kV)
PVP	4.0	25.0	20.0
PVP + AV	3.0	25.0	22.0
PVOH	8.0	15.0	15.0
PVOH + AV	8.0	15.0	15.0
BS	1.0	14.0	18.0
BS + AV	2.0	14.0	20.0
WPC	1.0	12.5	17.5
WPC + AV	1.0	12.5	17.5
maltodextrin	2.0	10.0	15.0
maltodextrin + AV	2.0	10.0	15.0

optimal conditions for each biopolymer solution during EHDP. All materials were processed at least 2 times at the optimized conditions, yielding similar morphological results. For the selected materials, various batches were produced to generate sufficient quantities for characterization and to achieve reproducibility.

Microscopy. The morphology of the obtained materials by EHDP was examined using scanning electron microscopy (SEM) with a S4800 from Hitachi (Tokyo, Japan). All materials were sputtered using a gold-palladium mixture under vacuum. Analysis was carried out at 10.0 kV, and estimation of the dimensions was performed by means of the Aperture software from Apple (Cupertino, CA, U.S.A.) using the SEM micrographs in their original magnification. In all cases, a minimum of 150 particles were analyzed to determine their sizes.

Ultraviolet (UV) Light Radiation. To accelerate the oxidation of AV and more rapidly evaluate the protecting effect provided by the biopolymers, the AV leaf juice and the selected AV-containing encapsulates were exposed to UV light radiation for a time span of 12 h. For this, an Ultra-Vitalux lamp from OSRAM Lighting S.L. (Madrid, Spain) was used. This operates with a power of 300 W that produces a blend of radiation very similar to that of natural sunlight, which is generated by a quartz discharge tube and a tungsten filament. The radiation of 315–400 nm after 1 h of exposure is of 13.6 W, and the radiation of 280–315 nm after 1 h of exposure is of 3.0 W.¹⁵

Infrared Spectroscopy. Fourier transform infrared (FTIR) spectra were collected coupling the attenuated total reflection (ATR) accessory Golden Gate of Specac, Ltd. (Orpington, U.K.) to a Bruker Tensor 37 FTIR equipment (Rheinstetten, Germany). Single spectra were collected by averaging 20 scans at 4 cm⁻¹ resolution of the materials in the wavelength range from 4000 to 400 cm⁻¹. To analyze the drying and stability of AV, the leaf juice was cast onto the ATR crystal to

reach approximately a 30 μm thickness film and repeated measurements were performed over time. Experiments were performed in duplicate.

Ultraviolet-Visible (UV-Vis) Spectroscopy. Stability of AV was determined by an UV-vis spectrophotometer NanoDrop ND1000 from Isogen Life Sciences (Utrecht, Netherlands). Absorbance was measured in the wavenumber range from 220 to 748 nm. Samples were measured after various UV light exposure times. The dried AV sample was prepared by casting the leaf juice onto a Petri dish, leaving it to dry in a desiccator at 0% relative humidity (RH) and room temperature until a constant dry mass of 2%. For the measurements, 400 parts per million (ppm) in distilled water of each solid was measured. At least 10 scans per sample were acquired.

Statistical Analysis. The solution properties and stability data were evaluated through analysis of variance (ANOVA) using Statgraphics Plus for Windows 5.1 from Manugistics Corporation (Rockville, MD, U.S.A.). Fisher's least significant difference (LSD) was used at the 95% confidence level ($p < 0.05$). Mean values and standard deviations were also calculated.

RESULTS AND DISCUSSION

Encapsulation of AV by EHDP. Table 3 summarizes the main solution properties of the different synthetic and naturally

that the AV leaf juice presents a certain ionic nature that increased solution conductivity. The highest values of conductivity were particularly observed for WPC and maltodextrin, showing values of 2.55 and 1.18 mS/cm, respectively. The other biopolymer solutions generated conductivity values lower than 1 mS/cm in all cases. The water-based PVP solution presented the lowest value, i.e., 0.04 mS/cm. In relation to viscosity and surface tension, it can be observed that the AV leaf juice had a negligible effect on these properties. This means that the biopolymers are the most influential elements in the solutions as expected, given their higher molar masses and mass quantities. All of these parameters are key during EHDP

Table 3. Solution Properties of PVP, PVOH, BS, WPC, and Maltodextrin with and without AV Used for EHDP^a

encapsulation system	conductivity (mS/cm)	viscosity (cP)	surface tension (mN/m)
PVP	0.04 (0.02) a	202.2 (1.6) a	30.4 (0.2) a
PVP + AV	0.27 (0.02) b	200.8 (1.2) b	29.5 (0.3) b
PVOH	0.29 (0.01) b	39.5 (0.4) f	44.4 (0.1) g
PVOH + AV	0.42 (0.01) d	39.6 (0.3) f	44.6 (0.2) g
BS	0.35 (0.02) c	65.5 (0.2) e	28.6 (0.2) c
BS + AV	0.51 (0.03) e	66.8 (0.1) d	28.2 (0.3) d
WPC	2.14 (0.02) h	10.9 (0.1) g	30.2 (0.1) a
WPC + AV	2.55 (0.03) i	11.2 (0.1) g	29.8 (0.1) b
maltodextrin	1.08 (0.02) f	80.6 (0.3) c	26.6 (0.1) f
maltodextrin + AV	1.18 (0.02) g	80.2 (0.2) c	27.2 (0.2) e

^a The results are expressed as the mean value (standard deviation), in which different letters indicate significant differences among the samples for the same solution property ($p < 0.05$).

occurring polymers solubilized in AV leaf juice prepared for EHDP. The table also includes the properties of the blank biopolymer solutions without AV, i.e., prepared in deionized water. As seen in the table, all biopolymer solutions based on AV leaf juice presented higher values of conductivity than their corresponding water-based solutions. This indicates

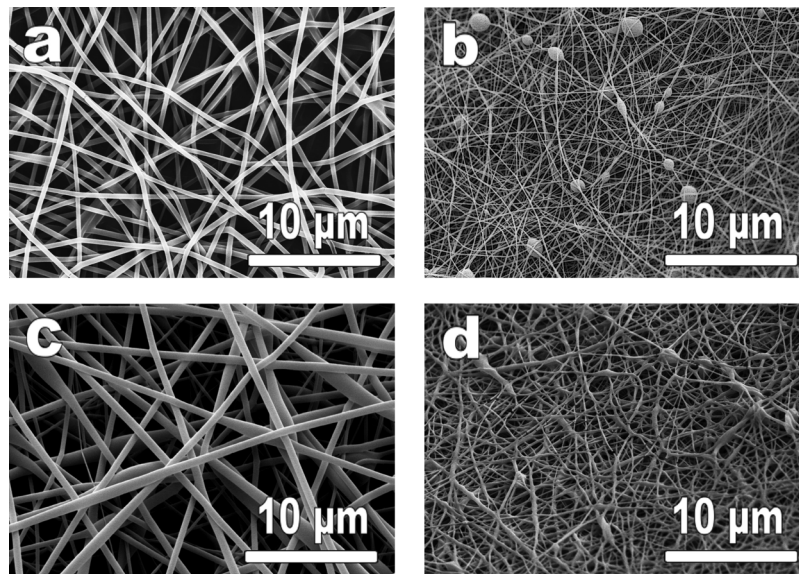
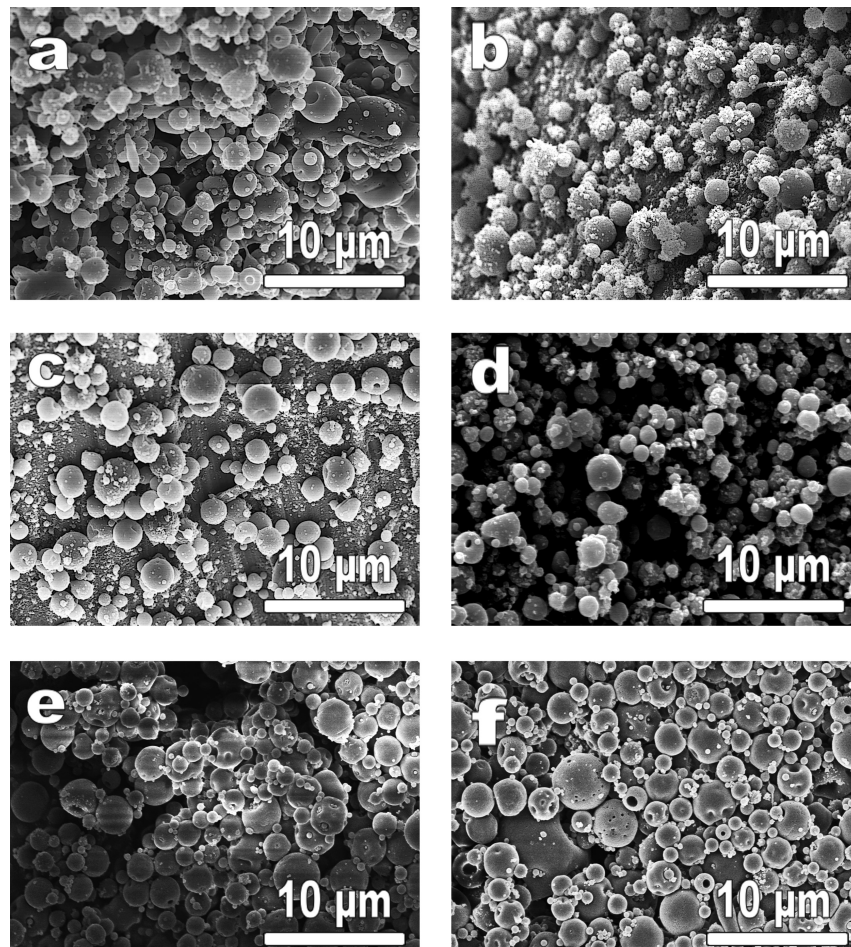


Figure 1. SEM images of electrospun fibers of (a) PVP, (b) PVP containing AV, (c) PVOH, and (d) PVOH containing AV. Scale markers are 10 μm.

Figure 2. SEM images of electrosprayed beads of (a) BS, (b) BS containing AV, (c) WPC, (d) WPC containing AV, (e) Maltodextrin, and (f) Maltodextrin containing AV. Scale markers are 10 μm.



because the use of polymer solutions with high viscosity and/or low surface tension tends to favor the formation of fibers.³⁰

Figure 1 shows the morphology of the synthetic polymer mats obtained by EHDP. In Figure 1a, it can be observed that the neat PVP solution produced ultrathin homogeneous nanofibers with diameters of approximately 500 nm. After AV encapsulation, shown in Figure 1b, it generated thinner PVP fibers with diameters below 200 nm but with the presence of some beaded regions. This interesting morphological change can be related to the above-observed increase in solution conductivity as a result of the ionic nature of the AV leaf juice. This increased the electrostatic repulsion between charges on the jet surface during EHDP, which induced the formation of thinner fibers but also impaired the formation of continuous fibers. A similar effect on the morphology of electrospun PVP materials has been recently observed for the encapsulation of microorganisms.³¹ In the case of neat PVOH, as shown in Figure 1c, electrospun fibers with a mean thickness between 600 nm and 1.5 μm were obtained. Thinner fibers of about 300 nm, with beaded regions in the range of 1–3 μm , can be seen in Figure 1d when PVOH encapsulated AV. However, some droplets or agglomerates can also be observed on the electrospun mat of PVOH nanofibers, which was not seen in the case of PVP nanofibers. This can be ascribed to the low viscosity observed for the AV-containing PVOH solution, which was approximately 5 times lower than that obtained for PVP. Higher viscosities, which are related to higher M_w and, hence, molecular entanglements, are typically needed during EHDP to produce fibers free of defects.³² These are thought to lead to higher viscoelastic forces that can resist the rapid changes in the polymer shape during EHDP. The larger tip-collector distance and lower flow rate required for the optimal processing of PVP could also contribute to its finer fiber formation.³⁰ For both synthetic polymers, the presence of some beaded regions within the nanofibers is probably related to instabilities during EHDP, which were triggered by the ionic nature of the AV leaf juice that significantly increased solution conductivity. In any case, other conditions different from the conditions selected resulted in processing instabilities or more ill-defined morphologies.

As opposite to synthetic polymers, which mainly presented a fiber-based morphology as a result of their high M_w , the use of food-grade polymers, also called hydrocolloids, typically resulted in beads or capsules. These can be seen in Figure 2. In general, spherical particles with a relatively narrow size distribution, including both small (<200 nm) and large (>3 μm) capsules, were produced. Similar morphologies have been recently observed for both electrospun carbohydrate-based²¹ and protein-based³³ materials. In Figure 2a, neat ultrathin capsules of BS obtained from pure water solutions can be observed. These show a bimodal distribution of sizes, in which ultrathin capsules with diameters as low as 300 nm coexist with some microcapsules with diameters between 1 and 3 μm . When BS was suspended in AV leaf juice, shown in Figure 2b, it

produced similar capsules with slightly lower diameters, ranging from 200 to 400 nm, for the smallest capsules, and from 1 to 2 μm , for the largest capsules. Unfortunately, excessive aggregation was also observed in the AV-containing BS capsules, probably as a result of moisture sorption from the ambient on the collector during EHDP. In relation to WPC, as shown in Figure 2c, EHDP of this food-grade polymer in pure water promoted the formation of ultrathin capsules with sizes ranging from 500 nm to above 2 μm . Similar to BS, when WPC was suspended in the AV leaf juice, it led to ultrathin capsules with slightly lower mean sizes and narrow size distribution. In particular, spherical particles of WPC ranging from 100 nm to 1 μm can be observed in Figure 2d. Interestingly, the resultant AV-containing WPC nanobeads seemed not to agglomerate on the collector. For maltodextrin, as shown in Figure 2e, the water suspension of this carbohydrate also produced round-like particles with different sizes, ranging from 300 nm to above 3 μm . In Figure 2f, it can be seen that maltodextrin electrospun from the AV leaf juice solution resulted in ultrathin capsules with similar morphologies. This can be related to the very low content of AV inside the carbohydrate, i.e., 2 wt %, which does not seem to affect the morphology of the maltodextrin capsules.

The formation of beads instead of fibers in these food hydrocolloids can be ascribed to the relatively high conductivity and low viscosity values generated by the solutions used for EHDP.^{21,34} It is also worth mentioning that the use of AV leaf juice instead of water led to a reduction in the mean sizes for most of the biopolymers, which was especially significant in the case of the electrospun fibers. This observation can be related to the higher content of encapsulated AV in the fibers than in the beads. This also correlates well with the above-observed increase in solution conductivity, even though other properties, such as viscosity and surface tension, were very dissimilar. This also suggests that very different polymer solutions in terms of viscosity, surface tension, and conductivity can be properly processed by EHDP, and these may have a combined effect on the resultant materials. In general, all obtained electrospun capsules have a physical appearance of easy-to-handle powder, whereas electrospun fibers are presented as continuous mats. In principle, the morphology of the electrospun capsules can result in more suitable uses as food additives, while the electrospun fiber mats can be of more interest in bioactive food packaging designs.^{13,14,35}

Encapsulation Stability of AV in Biopolymers. As a result of their ultrathin, disaggregated, and more regular morphology, application interest, and higher content of encapsulated AV, the electrospun PVP nanofibers and electrospun WPC nanobeads were selected as the encapsulating biopolymer-based structures to proceed with the stability analysis. These present a relatively dissimilar chemical structure and generated two opposite types of morphology.

Chemical assessment of the AV leaf juice was carried out by ATR-FTIR spectroscopy. This technique has been

successfully used in previous studies to determine the chemical composition of encapsulated bioactive compounds in electrosprayed matrices of different biopolymers.^{20,27} Figure 3 shows the FTIR spectra of the AV leaf juice, dried AV, and dried AV exposed to UV light for a span time of 12 h. In relation to the as-received AV leaf juice, it showed a broad and intense O-H stretching band in the 3000–3700 cm^{-1} range and the bending mode band of free water at $\sim 1635 \text{ cm}^{-1}$. This confirms that the AV leaf juice is highly hydrated. The presence of the highest intensity band, centered at approximately 3450 cm^{-1} , has been assigned to the stretching of -OH groups of different carbohydrate monomers (e.g., galacturonic acid, mannose,^{36–38} and uronic acid) and to the presence of hydrogen-bonded N-H stretching of amino acids.³⁹ These functional groups provide an interface for the interaction of polysaccharide chains in AV with other molecules via hydrogen bonding as a result of dipole-dipole attraction forces.⁴⁰

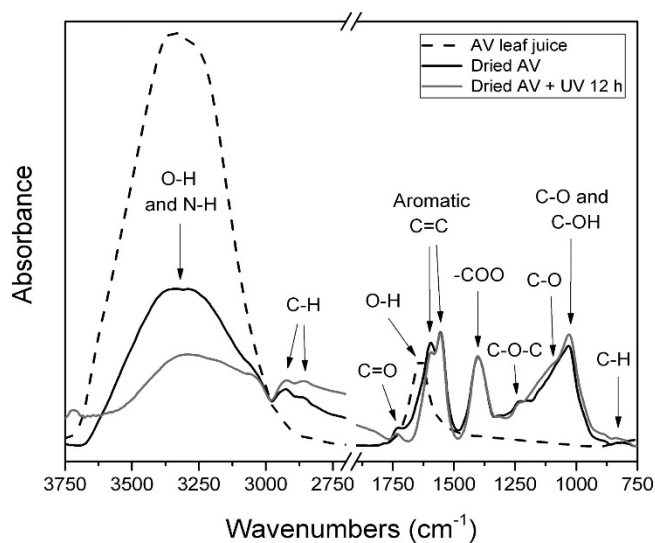


Figure 3. FTIR spectra of AV leaf juice, dried AV, and dried AV exposed to UV light for 12 h. Arrows indicate the bands discussed in the text.

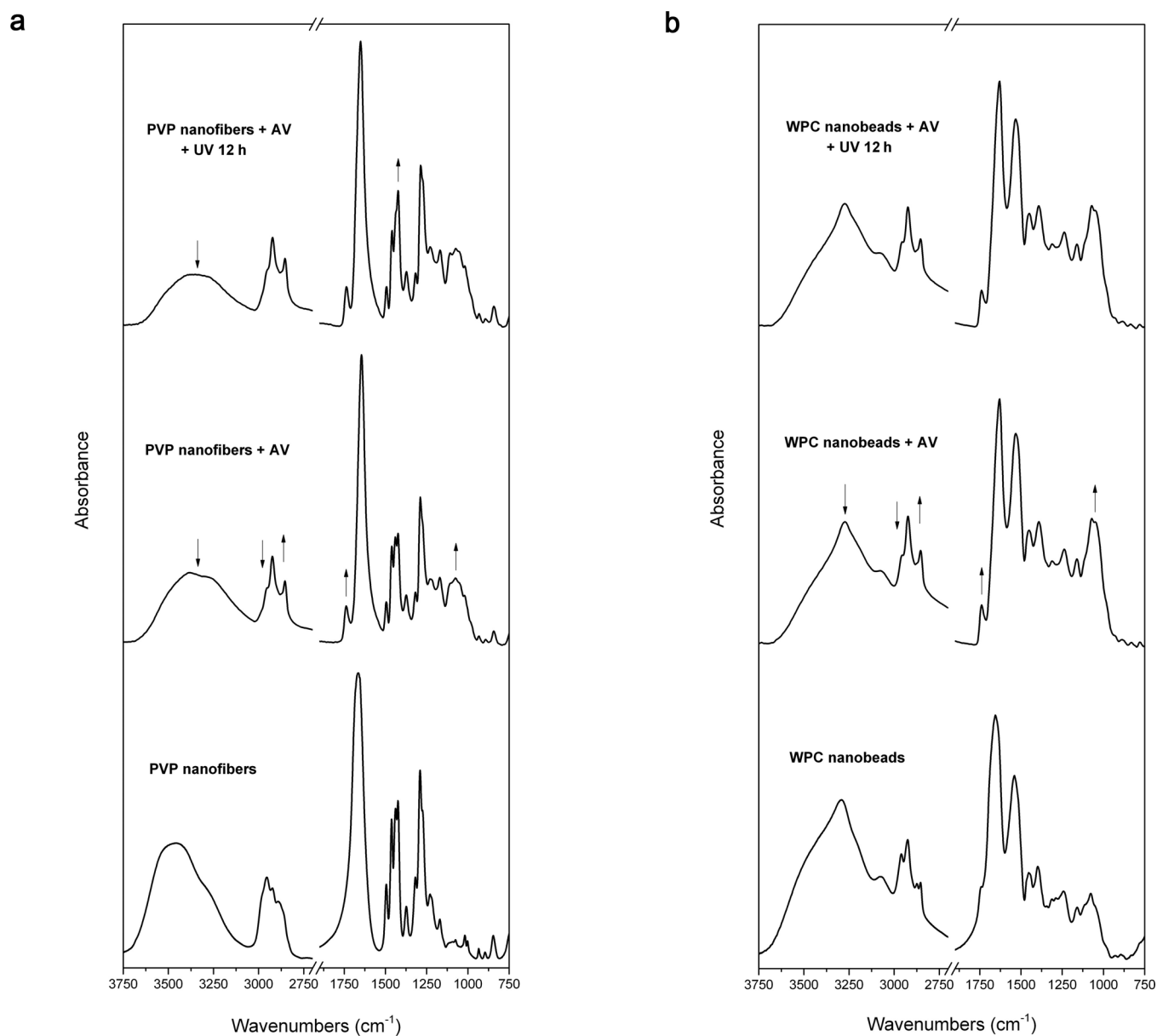


Figure 4. (a) FTIR spectra, from bottom to top, of PVP nanofibers, PVP nanofibers containing AV, and PVP nanofibers containing AV exposed to UV light for 12 h. (b) FTIR spectra, from bottom to top, of WPC nanobeads, WPC nanobeads containing AV, and WPC nanobeads containing AV exposed to UV light for 12 h. Arrows indicate the evolution of the bands.

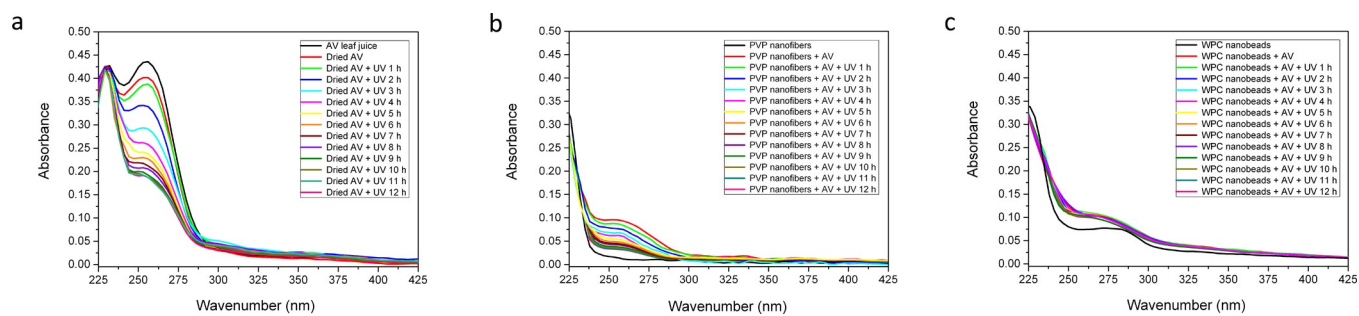


Figure 5. (a) UV-vis spectra of AV leaf juice and dried AV exposed to UV light, (b) UV-vis spectra of PVP nanofibers and PVP nanofibers containing AV exposed to UV light, and (c) UV-vis spectra of WPC nanobeads and WPC nanobeads containing AV exposed to UV light. UV-vis spectra were collected for times of UV light exposure from 0 to 12 h.

As said, once the AV leaf juice is dried, the main O–H band considerably reduced its intensity and moved down to ~ 3290 cm^{-1} . This suggests the presence of phenolic groups in AV based on anthraquinones (e.g., aloin and emodin),^{28,41} which typically contain hydroxyl groups (–OH) bonded directly to an aromatic hydrocarbon group, although the presence of remaining water cannot be excluded. Two new bands were formed at ca. 2922 and 2861 cm^{-1} that can be attributed to the C–H symmetric stretching (ν_s) and asymmetric stretching (ν_{as}) vibrations of methylene (CH_2), respectively.⁴² These bands would indicate the presence of long aliphatic (–CH) chains in AV.³⁹ The existence of a low intense carbonyl stretching band ($\text{C}=\text{O}$) at 1742 cm^{-1} and a C–O–C stretching vibration band at 1245 cm^{-1} , which are probably related to methyl acyl groups (– COCH_3), suggests the presence of O-acetyl ester.⁶ Two high characteristic bands potentially ascribed to aromatic double bonds ($\text{C}=\text{C}$) were also shown at ca. 1547 and 1604 cm^{-1} , which have been reported to carvone and limonene, respectively, in gel polysaccharide from AV.^{43–45} These $\text{C}=\text{C}$ stretching bands can further indicate the additional presence of vinyl ether and aloin compound.³⁹ The high intense peak at 1402 cm^{-1} can be assigned to symmetrical –COO stretching of carboxylate compounds. The shoulder peak at about 1075 cm^{-1} has been previously related to C–O stretching associated with acemannan³⁶ and rhamnogalacturonan,³⁸ which are side-chain constituents of pectins. The high intense band centered at 1031 cm^{-1} is considered to arise from the C–O and C–OH bonds of the glucan units in AV gel polysaccharides.⁴⁶ Finally, the low but broad absorption band in the range 900–800 cm^{-1} is ascribed to the C–H out-of-plane deformation of the pyranoside ring and mannose.⁴⁷

After 12 h of UV light exposure on the ATR plate, some relevant changes can be observed in the FTIR spectrum of the non-encapsulated dried AV. The main change is related to a further decrease of the broad O–H band. This change has been primarily ascribed to the oxidation of anthraquinones.⁴⁸ This is further supported by the decrease of the $\text{C}=\text{C}$ stretching band at 1604 cm^{-1} , which can be related to the oxidation of the aloin compound accompanied by the loss of limonene. In addition, the decrease in the peak intensity centered at 1742 cm^{-1} possibly corresponds to the deacetylation of acemannans.⁴⁰ This process is known to particularly contribute to the solidification of the AV gel and its loss of functional properties.⁴⁹ Instead, one can observe an absorption increase in the C–H alkyl stretching vibration band centered at 2861 cm^{-1} , accompanied by a further intensification of the C–O and C–OH groups at 1031 cm^{-1} . These latter changes mostly depict the contribution of highly stable monosaccharide units in the branched regions, such as galactose and glucan.^{37,38}

Figure 4 shows the FTIR spectra of the neat biopolymers and the encapsulated AV in the electrospun PVP nanofibers and WPC nanobeads, before and after UV light exposure. The evolution of some of the fingerprint bands found in the FTIR spectra of the non-encapsulated AV, shown in previous Figure 3, is marked with arrows in these spectra. In Figure

4a, a comparison of the FTIR spectra of neat PVP nanofibers versus PVP nanofibers containing AV clearly shows a reduction and shift of the O–H stretching vibration band of the biopolymer from ~ 3480 to 3370 cm^{-1} . On the one hand, this indicates that resultant PVP nanofibers could potentially retain a certain amount of water after EHDP. On the other hand, intra- and intermolecular hydrogen bonding are expected to occur among the biopolymer chains as a result of high hydrophilic forces with free water molecules and/or OH-based compounds of AV. The peak seen in neat PVP nanofibers at 2957 cm^{-1} is hardly distinguished after the introduction of AV, which is probably related to the high absorption of the OH stretching of AV hydroxyl groups. A similar effect was recently observed for electrospun AV-loaded PVOH nanofibers.²⁸ The addition of AV also shifted the carbonyl ($\text{C}=\text{O}$) stretching band from

1668 to 1651 cm^{-1} . This potentially suggests high intermolecular secondary interactions between carbonyl oxygen on the PVP chain, which is attached to the pyrrolidone rings, and hydroxyl groups of AV compounds. The appearance of a new sharp absorbance peak at 1737 cm^{-1} confirms the presence of ester components of AV in the nanofibers. The intense increase of the absorption peaks observed in the region of 1100–1000 cm^{-1} can be due to the C–O stretching of polysaccharides of AV, which was absent in the neat biopolymer spectrum. Interestingly, the FTIR spectrum of the AV-containing PVP nanofibers exposed to UV light also indicates certain changes in relation to the unexposed nanofibers. In particular, an additional reduction of the 3370 cm^{-1} O–H band was combined with a considerable increase of the bands in 1450–1400 cm^{-1} . The latter change can be related to an absorbance increase of the CH_2 bending vibrations of hydrocarbons of polysaccharides in AV.

For WPC, as seen in Figure 4b, the FTIR spectrum of the AV-loaded nanobeads also shows a reduction in the O–H band that was accompanied by a shift from ~ 3295 to 3270 cm^{-1} . This fact provides evidence of a certain hydrogen bond formation between the polysaccharides of AV and the –OH and – NH_2 terminal groups of the protein. Similar to PVP nanofibers, changes in the C–H stretching vibration bands in the range of 3000–2800 cm^{-1} after AV encapsulation were very significant. Incorporation of AV also generated a displacement toward lower wavenumbers of the amide I and II bands of the protein, particularly from 1656 to 1628 cm^{-1} and from 1540 to 1527 cm^{-1} , respectively. A similar effect was recently reported for electrospun lycopene-containing WPC capsules,⁵⁰ in which the shift of these amide bands was related to changes in the in-plane N–H and C–N vibrations. These changes suggest a considerable chemical or physicochemical interaction between the protein and encapsulated AV. In addition, a new prominent sharp peak was also observed in the spectrum of the AV-loaded WPC nanobeads at 1737 cm^{-1} . This may be due to the formation of new amide or ester linkages between the amino and carboxyl groups of both components. Additionally, a new group of C–O bands appeared in the 1100–1000 cm^{-1} range, which

can be related to esters and phenols of AV compounds. Interestingly, no relevant changes were noticeable in the AV-containing WPC nanobeads after UV light exposure. Consequently, these chemical changes confirm the successful encapsulation of the bioactive in both biopolymer matrices. However, these also suggest that the chemistry of AV compounds encapsulated in the PVP nanofibers changed during the UV light treatment, while these remained stable in the WPC nanobeads.

Stability of the AV-Containing Encapsulates against UV Light. In addition, to handle, store, and process the bioactive in a more appropriate dry form, another important purpose of encapsulation is to effectively protect the bioactive materials. The assessment of the protection of the two selected encapsulated systems was determined by UV-vis spectrophotometry during accelerated exposure to a strong UV light source for 12 h. Figure 5 shows the UV-vis spectra of the nonencapsulated AV leaf juice, AV-loaded PVP nanofibers, and AV-loaded WPC nanobeads as a function of the UV light exposure time. From observation of Figure 5a, it can be seen that AV presents two main intense absorption bands at 229 and 256 nm wavelength. The latter band can be associated from the results of this work to the bioactive degradation, and it was used to monitor aging in the AV. This band was seen to reduce absorption to some extent after the drying process. This suggests that both processes, i.e., drying and degradation, seem to occur simultaneously in AV. This observation and the fact that, after EHDP, the 256 nm absorption AV band was somewhat higher highlight the first benefit of this process versus conventional drying on the bioactive. Thus, EHDP avoided premature degradation during drying because this is instantaneous and occurs at ambient conditions. After strong exposure to UV light, the intensity of the band at 256 nm decreased absorption to a considerable extent, suggesting AV degradation, as mentioned above. Panels b and c of Figure 5 show that, while PVP hardly showed any absorption in the UV-vis range screened, WPC did show some absorption between 250 and 300 nm, hence providing some inherent level of UV protection. The two spectra of the biopolymers showed the peak at 256 nm when AV is encapsulated, which also decreased absorption with UV exposure as a result of degradation of the encapsulated bioactive. However, while the band intensity reduction was very small in the AV-loaded WPC nanobeads, it became noticeably intense in the PVP

nanofibers. Figure 6 shows the evolution of the absorbance of the 256 nm band normalized for the AV content as a function of UV light exposure time. From this, it can be easily observed that the non-encapsulated AV degraded quickly during the accelerated UV light exposure, with the bioactive stability being noticeably reduced for the first 5 h of radiation (~10% of stability). In relation to both biopolymer matrices, WPC nanobeads clearly arrested the photo-oxidation of encapsulated AV. The bioactive remained stable in the protein capsules up to the first 6 h of UV light (stability of >95%), showing certain degradation after 12 h of exposure (~60% of stability). On the contrary, PVP nanofibers did not provide any relevant protection, which is also in accordance with the FTIR data described above. It is interesting to note that the AV encapsulated in the PVP nanofibers presented a similar profile of degradation kinetics than the non-encapsulated sample, showing no significant differences after 5 h of UV light exposure. This observation confirms that PVP is not able to provide any efficient protection for the bioactive. A similar low protecting effect was previously observed during the encapsulation of folic acid in electrosprayed starch capsules.²⁷ This observation was related to the unique tendency of the carbohydrate to sorb and retain moisture during the processing and degradation treatment. This phenomenon of sorbed moisture may also apply here because PVP is a readily water-soluble polymer and its FTIR spectrum revealed strong moisture sorption. However, because WPC is also a strong water-absorbing material, there must be other factors, such as the encapsulated AV concentration, which was higher in PVP, and probably more importantly the higher gas barrier and UV absorption behavior of WPC. In addition, the PVP nanofibers may also have present some reactivity with the AV components because many more changes were observed in the FTIR spectra for this encapsulation system.

The present results indicate that the obtained contents of AV remained comparatively much more stable in WPC nanobeads. Whey protein is well-known to present a high barrier to oxygen and organic vapors,⁵¹ which would delay the oxidation process. Beyond these considerations, the high protection may also be contributed by the UV absorption capacity of the protein in the low UV range, as seen in Figure 5c. In this sense, it has been reported that aromatic amino acid residues, tyrosine and

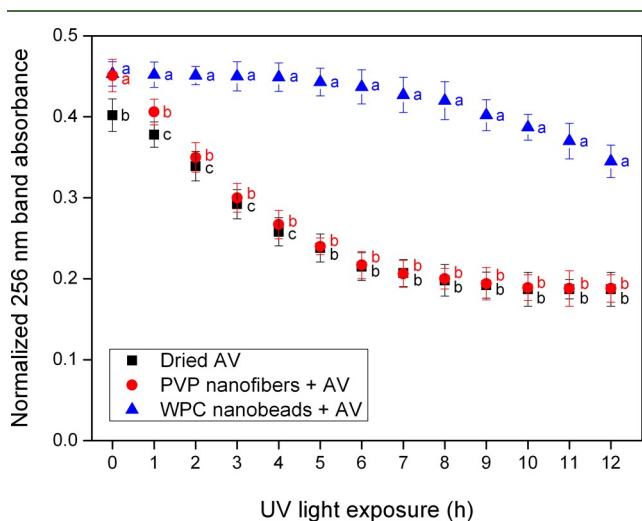


Figure 6. Evolution of the normalized 256 nm band versus time of UV light exposure for AV leaf juice, PVP nanofibers containing AV, and WPC nanobeads containing AV. Absorbance was normalized to the encapsulated AV content. Different letters indicate significant differences among the samples at the same time of UV light exposure ($p < 0.05$).

tryptophan, present in the whey protein structure are able to absorb in the UVC range, i.e., 100–290 nm.⁵² These results correlate well with previous studies performed on the encapsulation of β -carotene⁵³ and other bioactives,²⁴ in which electrosprayed WPC capsules showed enhanced protection against photo-oxidation. The findings reported here are also supported by the above FTIR results, in which no chemical changes were observed in the AV-containing WPC nanobeads. Additionally, these observations are in line with the recent results obtained for electrosprayed ultrathin WPI-based capsules,⁵⁴ which showed optimal protection for epigallocatechin gallate (EGCG) against moisture, heating, and dissolution conditions. Overall, it can be considered that WPC electrospraying creates ultrathin closed capsules that efficiently encapsulate AV and protect it from UV light degradation.

In summary, solid-like materials made of AV leaf juice extracts certainly open up new applications in the food industry, and the results reported here provide evidence of the possibility to chemically preserve AV in a dry form through the electrospraying of food hydrocolloids. In particular, electrosprayed WPC nanobeads offer efficient protection to AV bioactive compounds against UV light exposure. This can be related to the ultrathin capsule-like morphology of the WPC capsules as well as the high UV absorption, oxygen barrier, and positive interactions of the protein with the hydrophilic components of AV. Therefore, encapsulation of AV in WPC nanocapsules performed by EHDP shows a great deal of potential in the design of functional foods and nutraceutical applications and also in bioactive packaging. Further studies will be focused on determining the stability of electrosprayed capsules made of food hydrocolloids containing different amounts of bioactive

components and at diverse storing conditions, such as high temperature and high or low humidity.

AUTHOR INFORMATION

Corresponding Author

*E-mail: lagaron@iata.csic.es.

The authors thank the Spanish Ministry of Economy and Competitiveness (MINECO, Project AGL2015-63855-C2-1-R) for financial support.

Notes: The authors declare no competing financial interest.

REFERENCES

- (1) Baruah, A.; Bordoloi, M.; Deka Baruah, H. P. Aloe vera: A multipurpose industrial crop. *Ind. Crops Prod.* 2016, 94, 951–963.
- (2) Gulia, A.; Sharma, H. K.; Sarkar, B. C.; Upadhyay, A.; Shitandi, A. Changes in physico-chemical and functional properties during convective drying of aloe vera (*Aloe barbadensis*) leaves. *Food Bioprod. Process.* 2010, 88, 161–164.
- (3) Vega, A.; Uribe, E.; Lemus, R.; Miranda, M. Hot-air drying characteristics of Aloe vera (*Aloe barbadensis* Miller) and influence of temperature on kinetic parameters. *LWT-Food Sci. Technol.* 2007, 40, 1698–1707.
- (4) Sanchez-Machado, D. I.; Lopez-Cervantes, J.; Sendon, R.; Sanches-Silva, A. Aloe vera: Ancient knowledge with new frontiers. *Trends Food Sci. Technol.* 2017, 61, 94–102.
- (5) Reynolds, T.; Dweck, A. C. Aloe vera leaf gel: A review update. *J. Ethnopharmacol.* 1999, 68, 3–37.
- (6) Nejatizadeh-Barandozi, F.; Enferadi, S. T. FT-IR study of the polysaccharides isolated from the skin juice, gel juice, and flower of Aloe vera tissues affected by fertilizer treatment. *Org. Med. Chem. Lett.* 2012, 2, 33.
- (7) Krokida, M.; Pappa, A.; Agalio, M. Effect of drying on Aloe's functional components. *Procedia Food Sci.* 2011, 1, 1523–1527.
- (8) Hamman, J. Composition and Applications of Aloe vera Leaf Gel. *Molecules* 2008, 13, 1599–1616.
- (9) Uslu, I.; Aytimur, A. Production and characterization of poly(vinyl alcohol)/poly(vinylpyrrolidone) iodine/poly(ethylene glycol) electrospun fibers with (hydroxypropyl)methyl cellulose and aloe vera as promising material for wound dressing. *J. Appl. Polym. Sci.* 2012, 124, 3520–3524.
- (10) Uslu, I.; Keskin, S.; Güll, A.; Karabulut, T. C.; Aksu, M. L. Preparation and properties of electrospun poly(vinyl alcohol) blended hybrid polymer with Aloe vera and HPMC as wound dressing. *Hacettepe J. Biol. Chem.* 2010, 38, 19–25.
- (11) Esmaeili, A.; Ebrahimzadeh, M. Preparation of Polyamide Nanocapsules of Aloe vera L. Delivery with In Vivo Studies. *AAPS PharmSciTech* 2015, 16, 242–249.
- (12) Esmaeili, A.; Ebrahimzadeh, M. Polymer-Based of ExtractLoaded Nanocapsules Aloe vera L. Delivery. *Synth. React. Inorg., Met. Org., Nano-Met. Chem.* 2015, 45, 40–47.
- (13) Echevoyen, Y.; Fabra, M. J.; Castro-Mayorga, J. L.; Cherpinski, A.; Lagaron, J. M. High throughput electro-

hydrodynamic processing in food encapsulation and food packaging applications: Viewpoint. *Trends Food Sci. Technol.* 2017, 60, 71–79.

(14) Torres-Giner, S.; Perez-Masiá, R.; Lagaron, J. M. A review on electrospun polymer nanostructures as advanced bioactive platforms. *Polym. Eng. Sci.* 2016, 56, 500–527.

(15) Fernandez, A.; Torres-Giner, S.; Lagaron, J. M. Novel route to stabilization of bioactive antioxidants by encapsulation in electrospun fibers of zein prolamine. *Food Hydrocolloids* 2009, 23, 1427–1432.

(16) de Freitas Zômpero, R. H.; Lopez-Rubio, A.; de Pinho, S. C.; Lagaron, J. M.; de la Torre, L. G. Hybrid encapsulation structures based on β -carotene-loaded nanoliposomes within electrospun fibers. *Colloids Surf., B* 2015, 134, 475–482.

(17) Anu Bhushani, J.; Anandharamakrishnan, C. Electrospinning and electrospraying techniques: Potential food based applications. *Trends Food Sci. Technol.* 2014, 38, 21–33.

(18) Esmacili, A.; Haseli, M. Electrospinning of thermoplastic carboxymethyl cellulose/poly(ethylene oxide) nanofibers for use in drug-release systems. *Mater. Sci. Eng. C* 2017, 77, 1117–1127.

(19) Alp Erbay, E.; Dağtekin, B. B. G.; Türe, M.; Yesilsu, A. F.; Torres-Giner, S. Quality improvement of rainbow trout fillets by whey protein isolate coatings containing electrospun poly(ϵ -caprolactone) nanofibers with *Urtica dioica* L. extract during storage. *LWT–Food Sci. Technol.* 2017, 78, 340–351.

(20) Torres-Giner, S.; Martinez-Abad, A.; Ocio, M. J.; Lagaron, J. M. Stabilization of a Nutraceutical Omega-3 Fatty Acid by Encapsulation in Ultrathin Electrosprayed Zein Prolamine. *J. Food Sci.* 2010, 75, N69–N79.

(21) García-Moreno, P. J.; Özdemir, N.; Stephansen, K.; Mateiu, R. V.; Echegoyen, Y.; Lagaron, J. M.; Chronakis, I. S.; Jacobsen, C. Development of carbohydrate-based nanostructures loaded with fish oil by using electrohydrodynamic processing. *Food Hydrocolloids* 2017, 69, 273–285.

(22) Stijnman, A. C.; Bodnar, I.; Hans Tromp, R. Electrospinning of food-grade polysaccharides. *Food Hydrocolloids* 2011, 25, 1393–1398. (23) Nieuwland, M.; Geerdink, P.; Brier, P.; van den Eijnden, P.; Henket, J. T. M. M.; Langelaan, M. L. P.; Stroeks, N.; van Deventer, H. C.; Martin, A. H. Food-grade electrospinning of proteins. *Innovative Food Sci. Emerging Technol.* 2013, 20, 269–275.

(24) Sullivan, S. T.; Tang, C.; Kennedy, A.; Talwar, S.; Khan, S. A. Electrospinning and heat treatment of whey protein nanofibers. *Food Hydrocolloids* 2014, 35, 36–50.

(25) Jung, J.-M.; Savin, G.; Pouzot, M.; Schmitt, C.; Mezzenga, R. Structure of Heat-Induced β -Lactoglobulin Aggregates and their Complexes with Sodium-Dodecyl Sulfate. *Biomacromolecules* 2008, 9, 2477–2486.

(26) Alting, A. C.; Weijers, M.; de Hoog, E. H. A.; van de Pijpekamp, A. M.; Cohen Stuart, M. A.; Hamer, R. J.; de Kruijff, C. G.; Visschers, R. W. Acid-Induced Cold Gelation of Globular Proteins: Effects of Protein Aggregate Characteristics and Disulfide Bonding on Rheological Properties. *J. Agric. Food Chem.* 2004, 52, 623–631.

(27) Perez-Masiá, R.; López-Nicolás, R.; Periago, M. J.; Ros, G.; Lagaron, J. M.; Lopez-Rubio, A. Encapsulation of folic acid in food hydrocolloids through nanospray drying and electrospraying for nutraceutical applications. *Food Chem.* 2015, 168, 124–133.

(28) Abdullah Shukry, N. A.; Ahmad Sekak, K.; Ahmad, M. R.; Bustami Effendi, T. J. Characteristics of Electrospun PVA-Aloe vera Nanofibres Produced via Electrospinning. In *Proceedings of the International Colloquium in Textile Engineering, Fashion, Apparel and Design 2014 (ICTEFAD 2014)*; Ahmad, M. R., Yahya, M. F., Eds.; Springer: Singapore, 2014; pp 7–11, DOI: 10.1007/978-981-287-0117_2.

(29) Serincay, H.; Özkan, S.; Yılmaz, N.; Kocyiğit, S.; Uslu, I.; Gürçan, S.; Arısoy, M. PVA/PAA-Based Antibacterial Wound Dressing Material with Aloe Vera. *Polym.-Plast. Technol. Eng.* 2013, 52, 1308–1315.

(30) Torres-Giner, S.; Gimenez, E.; Lagaron, J. M. Characterization of the morphology and thermal properties of Zein Prolamine nanostructures obtained by electrospinning. *Food Hydrocolloids* 2008, 22, 601–614.

(31) Libran, C. M.; Castro, S.; Lagaron, J. M. Encapsulation by electrospray coating atomization of probiotic strains. *Innovative Food Sci. Emerging Technol.* 2017, 39, 216–222.

(32) Torres-Giner, S.; Ocio, M. J.; Lagaron, J. M. Novel antimicrobial ultrathin structures of zein/chitosan blends obtained by electrospinning. *Carbohydr. Polym.* 2009, 77, 261–266.

(33) Gomez-Mascaraque, L. G.; Lopez-Rubio, A. Protein-based emulsion electrosprayed micro- and submicroparticles for the encapsulation and stabilization of thermosensitive hydrophobic bioactives. *J. Colloid Interface Sci.* 2016, 465, 259–270.

(34) Torres-Giner, S.; Ocio, M. J.; Lagaron, J. M. Development of Active Antimicrobial Fiber-Based Chitosan Polysaccharide Nanostructures using Electrospinning. *Eng. Life Sci.* 2008, 8, 303–314.

(35) Torres-Giner, S. Electrospun nanofibers for food packaging applications. *Multifunctional and Nanoreinforced Polymers for Food Packaging*; Woodhead Publishing Limited: Cambridge, U.K., 2011; pp 108–125, DOI: 10.1533/9780857092786.1.108.

(36) Ray, A.; Aswatha, S. M. An analysis of the influence of growth periods on physical appearance, and acemannan and elemental distribution of Aloe vera L. gel. *Ind. Crops Prod.* 2013, 48, 36–42.

(37) Swami Hulle, N. R.; Patrani, K.; Rao, P. S. Rheological Properties of Aloe Vera (*Aloe barbadensis* Miller) Juice Concentrates. *J. Food Process Eng.* 2014, 37, 375–386.

(38) Gentilini, R.; Bozzini, S.; Munarin, F.; Petrini, P.; Visai, L.; Tanzi, M. C. Pectins from Aloe Vera: Extraction and production of gels for regenerative medicine. *J. Appl. Polym. Sci.* 2014, 131, 39760.

(39) Jithendra, P.; Rajam, A. M.; Kalaivani, T.; Mandal, A. B.; Rose, C. Preparation and Characterization of Aloe Vera Blended Collagen/Chitosan Composite Scaffold for Tissue Engineering Applications. *ACS Appl. Mater. Interfaces* 2013, 5, 7291–7298.

(40) Lim, Z. X.; Cheong, K. Y. Effects of drying temperature and ethanol concentration on bipolar switching characteristics of natural Aloe vera-based memory devices. *Phys. Chem. Chem. Phys.* 2015, 17, 26833–26853.

(41) Nindo, C. I.; Powers, J. R.; Tang, J. Thermal Properties of Aloe Vera Powder and Rheology of Reconstituted Gels. *Trans. ASABE* 2010, 53, 1193–1200.

(42) Dignac, M. F.; Derenne, S.; Ginestet, P.; Bruchet, A.; Knicker, H.; Largeau, C. Determination of structure and origin of refractory organic matter in bio-epurated wastewater via

spectroscopic methods. Comparison of conventional and ozonation treatments. *Environ. Sci. Technol.* 2000, 34, 3389–3394.

(43) Ghayempour, S.; Montazer, M.; Mahmoudi Rad, M.

Simultaneous encapsulation and stabilization of Aloe vera extract on cotton fabric for wound dressing application. *RSC Adv.* 2016, 6, 111895–111902.

(44) Ghayempour, S.; Montazer, M.; Mahmoudi Rad, M.

Encapsulation of Aloe Vera extract into natural Tragacanth Gum as a novel green wound healing product. *Int. J. Biol. Macromol.* 2016, 93, 344–349.

(45) Brahmachari, G.; Banerjee, B. Facile synthesis of symmetrical bis(benzhydryl)ethers using p-toluenesulfonyl chloride under solventfree conditions. *Org. Med. Chem. Lett.* 2013, 3, 1–7.

(46) Kacuráková, M.; Capek, P.; Sasinková, V.; Wellner, N.; Ebringerova, A. FT-IR study of plant cell wall model compounds: Pectic polysaccharides and hemicelluloses. *Carbohydr. Polym.* 2000, 43, 195–203.

(47) Yan, J.-C.; Cui, C.-Y.; Zhang, Y.; Chu, R.-H. Separation, Purification and Structural Analysis of Polysaccharides from Aloe. *Chem. J. Chin. Univ.* 2003, 24, 1189–1192.

(48) Fanchiang, J.-M.; Tseng, D.-H. Degradation of anthraquinone dye C.I. Reactive Blue 19 in aqueous solution by ozonation. *Chemosphere* 2009, 77, 214–221.

(49) Femenia, A.; García-Pascual, P.; Simal, S.; Rossello, C. Effects of heat treatment and dehydration on bioactive polysaccharide acemannan and cell wall polymers from Aloe barbadensis Miller. *Carbohydr. Polym.* 2003, 51, 397–405.

(50) Perez-Masiá, R.; Lagaron, J. M.; Lopez-Rubio, A. Morphology and Stability of Edible Lycopene-Containing Micro- and Nanocapsules Produced Through Electrospraying and Spray Drying. *Food Bioprocess Technol.* 2015, 8, 459–470.

(51) Mate, J. I.; Krochta, J. M. Comparison of Oxygen and Water Vapor Permeabilities of Whey Protein Isolate and β -Lactoglobulin Edible Films. *J. Agric. Food Chem.* 1996, 44, 3001–3004.

(52) Li, Y.; Jiang, Y.; Liu, F.; Ren, F.; Zhao, G.; Leng, X. Fabrication and characterization of TiO₂/whey protein isolate nanocomposite film. *Food Hydrocolloids* 2011, 25, 1098–1104.

(53) Lopez-Rubio, A.; Lagaron, J. M. Whey protein capsules obtained through electrospraying for the encapsulation of bioactives. *Innovative Food Sci. Emerging Technol.* 2012, 13, 200–206.

(54) Paximada, P.; Echegoyen, Y.; Koutinas, A. A.; Mandala, I. G.; Lagaron, J. M. Encapsulation of hydrophilic and lipophilized catechin into nanoparticles through emulsion electrospraying. *Food Hydrocolloids* 2017, 64, 123–132.